Process controls on regional flood frequency: Coefficient of variation and basin scale

Günter Blöschl and Murugesu Sivapalan[1]

Institut für Hydraulik, Gewässerkunde und Wasserwirtschaft, Technische Universität Wien, Vienna, Austria

Abstract. The coefficient of variation (CV) of maximum annual floods is examined to understand the effects of process controls and catchment size. A derived flood frequency model is used to interpret data from 489 catchments in Austria. At the core of process controls appears to be the interaction of catchment response time and storm duration, but the magnitude is not large, and often this interaction is hidden by other processes. The dependence of rainfall intensity and duration is clearly very important and reduces CV significantly. Increasing channel travel times with catchment scale tend to translate into decreasing CVs with area for small catchments while they tend to translate into increasing CVs with area for larger catchments. Nonlinear runoff processes, including threshold effects, is the main mechanism for increasing CV. They give rise to complex patterns in the relationship between CV and area. Base flow has been used as a surrogate for a number of processes, such as seasonality of streamflow. It always decreases CV and, in particular, leads to a significant decrease of CV with area. Both the observed tendency of CV to decrease with area and the scatter in the data are the result of a complex interplay of a number of processes which allows various alternative interpretations. Depending on which processes dominate under a particular hydrologic regime, different patterns arise. It appears that the explanations of the relationship between CV and catchment scale suggested in the literature are too simplistic. The case is made for using the concept of hydrologic regimes and process studies of the type presented here to help delineate homogeneous regions for regional flood frequency analyses in a physically consistent way.

1. Introduction

Regional analyses of floods have been and continue to be of great significance in various hydrologic contexts. In a practical context they are widely used to estimate floods at ungauged sites and to enhance the reliability of flood estimates at gauged sites [*Cunnane*, 1985]. In a more theoretical context they can contribute to advance our understanding of the spatial variability and scaling of hydrologic fluxes [*Gupta et al.*, 1994; *Blöschl and Sivapalan*, 1995; *Blöschl*, 1996]. One of the key parameters in regional flood frequency analyses is the coefficient of variation (CV), which is the ratio of standard deviation and mean of a series of flood peaks. The CV is a measure of the steepness of the flood frequency curve. A particularly intriguing question, from a regional point of view, is the relationship between CV and basin scale and the nature of the processes that control this relationship. It is clear that a deeper understanding of process controls is highly relevant to regional flood frequency analyses, but so far, not much work has been devoted to this subject matter.

Regional flood frequency procedures deal with the relationship between CV and basin scale in different ways. Some procedures, such as quantile regression methods, use empirical relationships. Other procedures, such as the index flood method [*Dalrymple*, 1960], are based on the concept of homo-

geneous regions, and the CV in any such region is assumed to be constant rather than a function of catchment area [*Gupta et al.*, 1994]. This is because in the index flood method, all flood frequency curves (and hence all standard deviations) in a region are scaled by the mean annual flood to produce one characteristic regional curve.

Although the index flood method has been highly successful in practice, there is data evidence which suggests that, in many cases, there does exist a significant relationship between CV and catchment area. Data evidence comes from two avenues of enquiry: (1) quantile-based analyses and (2) moment-based analyses.

1. Quantile-based analyses. Relationships between floods of a given return period (i.e., flood quantiles) and catchment area are often framed in a power law of the form

$$Q_T = c(T)A^{\theta(T)} \qquad (1)$$

where Q_T are the flood quantiles, c is a constant, T is the return period, A is catchment area, and θ is an exponent. A number of studies, for different climates, have shown a tendency of θ to decrease with return period [e.g., *Kölla*, 1986]. Small floods, on the order of the long-term average discharge, are associated with θ close to unity due to mass balance. Mean annual floods ($T = 2.3$ years) typically give θ from 0.6 to 0.9 [e.g., *Gupta and Dawdy*, 1995], while the envelopes of maximum observed floods (equivalent to T of several hundred years) tend to yield significantly lower exponents of 0.4 to 0.6 [e.g., *Wundt*, 1950; *Gutknecht and Watzinger*, 1995]. The low exponents are usually attributed to the limited spatial extent of extreme events. It is clear that the decrease of θ with return period implies a decrease of CV with catchment area (see, e.g., work by *Gupta et al.* [1994] for a discussion).

---

[1]On leave from Centre for Water Research, University of Western Australia, Nedlands, Australia.

2. Moment-based analyses. A recent example of a moment-based analysis has been provided by *Smith* [1992] for the central Appalachian region. *Smith* [1992] suggested that there may exist a consistent relationship between CV and catchment scale. Average CVs in the region appeared to increase between 1 and 100 km² (CV = 0.7 to 1.2) but to decrease between 100 and 25,000 km² (CV = 1.2 to 0.6), which implies a peak in average CV at a catchment size of 100 km². The CVs of individual catchments ranged from 0.4 to 1.9.

There have been a number of potential explanations for *Smith*'s [1992] data. Smith suggested two alternative hypotheses. First, the data of the small basins may be unrepresentative owing to possible systematic errors in stream gauging or sampling artifacts, which would suggest that CV always decreases with catchment scale. Second, the peak may be real and is related to the organization of extreme storm rainfall and the downstream development of the channel/floodplain system. *Gupta and Dawdy* [1995] provided an alternative interpretation. On the basis of preliminary rainfall runoff simulations they suggested CV, at small catchment scales below a critical catchment size, to be controlled by basin response. Based on a comparison of snowmelt and rainfall dominated catchments they suggested CV at large basin scales to be controlled by the scaling behavior of rainfall. A further interpretation, based on a derived flood frequency model, has been furnished by *Robinson and Sivapalan* [1997]. They suggested that the increase in CV in small catchments is due to the interaction between timescales of storm duration and catchment response, while the decrease in CV in large catchments is due to the spatial scaling of rainfall. However, their derived flood frequency model was very simple and did account for neither nonlinear runoff generation processes nor the interdependence between storm duration and intensity. Also, their simulated CVs were significantly larger than the data reported by *Smith* [1992], and their rate of change of CV with catchment size was very small (CV = 1.17 at 1 km², 1.32 at 200 km², and 1.2 at 10,000 km²).

The aim of this paper is to investigate the relationship between CV and catchment area in more detail and to analyze the process controls on this relationship. We use a derived flood frequency model (M. Sivapalan et al., unpublished manuscript) to interpret flood data from 489 catchments in Austria. The emphasis is on understanding process controls, which is in the spirit of *Klemeš* [1993], M. Sivapalan et al. (unpublished manuscript) and G. Blöschl and M. Sivapalan (unpublished manuscript). Because of the emphasis on process understanding, we use typical model parameters. While we do not claim that these parameters are valid for all the catchments considered in this paper, we do believe they allow insight into the interplay of processes that typically occur in this type of catchments.

The paper is organized as follows: In section 2, data evidence is given and hydrologic regimes in Austria are discussed. Section 3 presents a brief overview of the derived flood frequency model used. A "first guess" to mimic the observed data in terms of their CV is given that uses the complete model. However, to allow insight into the process controls, section 4 starts with a very simple derived flood frequency model, and model components are added in steps. At each step the effect of the additional process is assessed. Processes examined include the interaction of storm duration and catchment response time (section 4), nonlinearity in runoff generation (section 5), and hydrologic regimes (section 6).
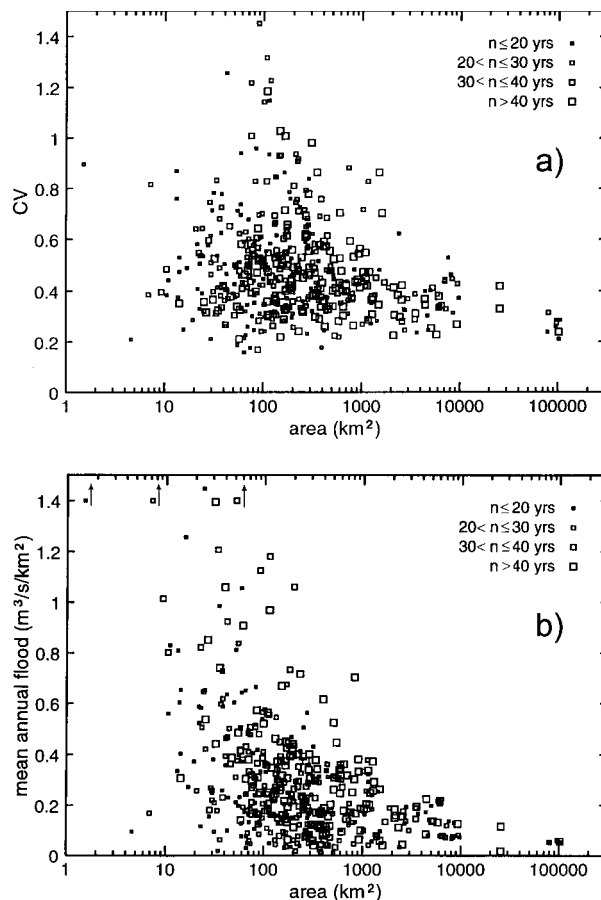

Figure 1. Coefficient of variation and mean of maximum annual floods per unit area for 489 catchments in Austria plotted versus catchment area. Observation periods, *n*, are shown, and the last year included is 1991.

2. Data Evidence

The flood data used in this study are annual series from 489 catchments in Austria. These data represent a complete set of catchments for which discharge data are published by the Federal Hydrographic Office of Austria. The data set contains 134 catchments with more than 40 years of observation; the minimum observation period is 15 years. Catchment sizes vary from 1 to 100,000 km². Figure 1 shows CVs and mean annual floods per area plotted versus catchment area. CVs vary from 0.2 to 1.4 (Figure 1a). The largest values stem from catchments with less than 30 years of record. On average, CVs are slightly lower than those reported by *Smith* [1992], but the general pattern is similar. There is a general tendency of CV to decrease with catchment area. Although maximum CVs appear at a catchment scale of 100 km², as in Smith's data, there is no clear evidence of CV to increase with catchment area at scales below 100 km². Mean annual floods per area (Figure 1b) vary from 0.02 to 2 m³/s/km² which is a larger range than that of CV. Despite the large scatter, there is a clear tendency of mean annual floods per area to decrease with catchment area. Fitting a power law to the data yields an exponent of −0.25, which corresponds to an exponent of $\theta = 0.75$ for the relationship between mean annual floods and area (equation (1)). This is well within the range of exponents reported in the literature,
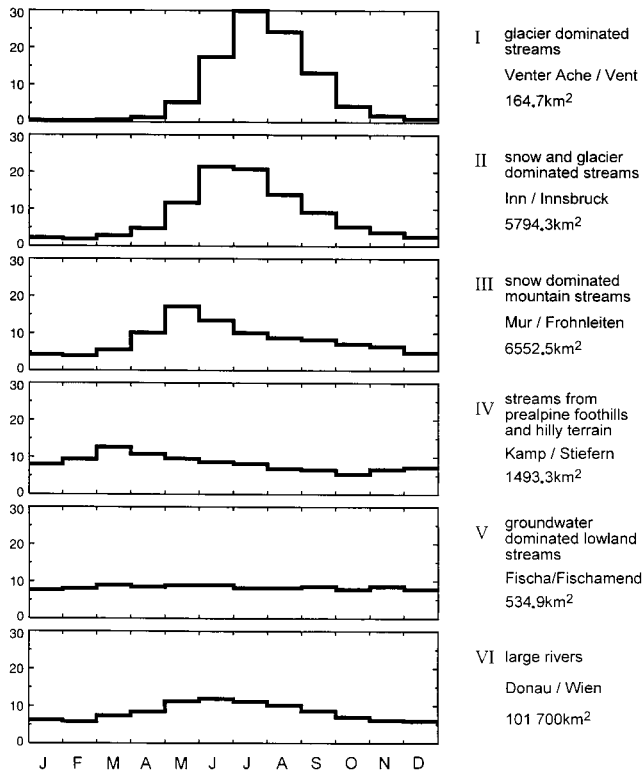
Figure 2. Regime classification for Austrian streams according to *Kresser* [1981]. Examples for each regime are given. Graphs show long-term mean monthly flows as percentage of annual flows. Redrawn after *Kresser* [1981].

which is about 0.6 to 0.9 [e.g., *Gupta and Dawdy*, 1995; *Kölla*, 1986].

Part of the scatter in Figure 1 stems from differences in physiographic characteristics between catchments, which are reflected in different hydrologic regimes. *Kresser* [1981] proposed a classification of hydrologic regimes in Austria that is based on the seasonal variability of streamflow (Figure 2). There are six main regimes. Catchments representative of these regimes are given in Figure 2 for illustration. In regime I, streamflow is glacier dominated, and floods mainly occur in summer, when streamflow is generally high. Fast surface runoff from glaciers during convective storms may be important for

flooding. Regime III is snowmelt dominated, and, again, floods often occur in summer, but both convective and synoptic events may be important; also, the seasonal variability is not as pronounced as in regime I and runoff response is often slower. Regime II lies between I and III. All of the regimes I to III relate to Alpine catchments. Regime IV represents streams from prealpine foothills and hilly terrain, where floods may occur at any time of the year and where a range of climatic and runoff mechanisms may be important. Regime V refers to groundwater-dominated lowland streams, with very slow runoff response and, consequently, very low flood peaks. Finally, regime VI represents streamflow from large river basins and contains the combined effects of the other regimes.

3. Derived Flood Frequency Model

This is a brief summary of the derived flood frequency model of M. Sivapalan et al. (unpublished manuscript) and G. Blöschl and M. Sivapalan (unpublished manuscript), which is used here. The model builds on the paradigm of *Eagleson's* [1972] approach. It mainly consists of (1) a rainfall model, (2) a runoff model, and (3) their combination in an analytical flood frequency framework (Figure 3). The model is event based. M. Sivapalan et al. (unpublished manuscript) identified, by a downward approach [*Klemeš*, 1983], three phenomena that were particularly important: (1) within-storm rainfall patterns, (2) multiple events, and (3) increasing runoff coefficients with increasing storm depth. M. Sivapalan et al. (unpublished manuscript) tested the model based on extensive rainfall and runoff observations in four Austrian catchments.

3.1. Rainfall Model

Catchment idf curves [*Sivapalan and Blöschl*, 1997] are used to specify catchment-average rainfall intensity as a function of storm duration and return period. These are based on a combination of point idf curves with the spatial correlation structure of rainfall through a variance reduction factor; idf curves are conditional cumulative distributions of rainfall intensity, conditioned on rainfall duration. The approach of deriving catchment idf curves consists of four steps [*Sivapalan and Blöschl*, 1997]. In the first step a parent distribution of the point rainfall process is specified. In the second step this point process is averaged over a catchment area. In the third step the parent distribution of the areally averaged rainfall process is
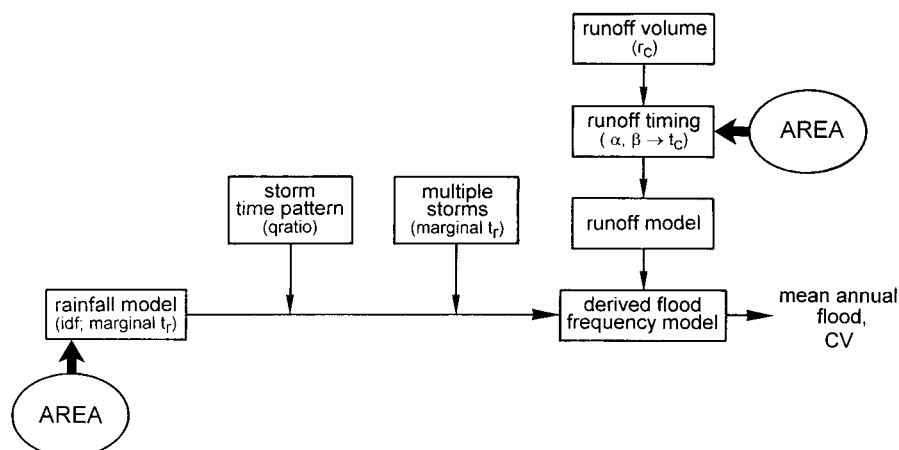

Figure 3. Schematic of the derived flood frequency model.

transformed to the corresponding extreme value distribution using the asymptotic extreme value theory of *Gumbel* [1958]. In the fourth and final step the extreme value distribution derived above is matched, for the particular case of zero catchment area, with observed extreme value distributions of point rainfall (i.e., point idf curves), which then yields the parameters of the catchment idf curves. In this approach the CV of catchment rainfall, for a given duration, decreases slightly with catchment area. Selection of the correlation structure has been guided by both rainfall data [*Sivapalan and Blöschl*, 1997] and a comparison of simulated and observed mean annual floods presented later in this paper. The correlation structure is represented by

$$\rho(h) = 0.9 \times \exp\left(\frac{-h}{5}\right) + 0.1 \times \left(\frac{-h}{50}\right) \tag{2}$$

where ρ is the correlation coefficient and h is the spatial lag (in kilometers). As noted by *Vanmarcke* [1983, p. 226] and *Gelhar* [1993, p. 296] this type of composite correlation model closely resembles a fractal model while being more convenient mathematically. Storm durations, t_r, are specified by a marginal density function, f_1, according to a Weibull distribution:

$$f_1(t_r) = \frac{c}{\delta}\left(\frac{t_r - a}{\delta}\right)^{c-1} \exp\left[-\left(\frac{t_r - a}{\delta}\right)^c\right] \tag{3}$$

Parameters a and c were set to $a = 1.5$ hours and $c = 0.80$. The average storm duration, δ, was set to $\delta = 48$ hours to allow for multiple storm events (M. Sivapalan et al., unpublished manuscript). If two rainstorms are separated by a gap that is short compared to the characteristic time of the direct catchment response, the hydrograph may show multiple peaks. These two events then should be treated together. M. Sivapalan et al. (unpublished manuscript) introduced an "effective storm duration," which is larger than the single storm duration and is an approximate representation of what the catchment "sees" in the case of multiple peaks. The selection of $\delta = 48$ hours in this paper is based on this notion of an "effective storm duration." It should be noted that the model assumes storm duration to be independent of the spatial correlation structure of rainfall.

Within-storm time patterns are parameterized by the ratio of peak flow with and without time patterns, q_{ratio}, according to

$$q_{\text{ratio}} = 1.0 \qquad t_r/t_c < 0.2$$

$$q_{\text{ratio}} = 1 + 0.1 \times \left[\log\left(\frac{t_r}{t_c \times 0.2}\right)\right]^{2.3} \qquad \text{otherwise} \tag{4}$$

where t_r is storm duration and t_c is the characteristic catchment response time (M. Sivapalan et al., unpublished manuscript). This relationship was found by assuming a number of dimensionless time patterns of within-storm rainfall (i.e. mass curves) [*Huff*, 1967] that are typical of Austrian conditions and convoluting each of them with a runoff model represented as a linear reservoir with t_c. From this, M. Sivapalan et al. (unpublished manuscript) estimated the peak discharge and q_{ratio} as the ratio of the peak discharges for within-storm time patterns to those of the rectangular (constant) time pattern, for the same duration. As a last step, M. Sivapalan et al. (unpublished manuscript) fitted an analytical relationship (Eq. 4) to the computed values. Equation (4) corresponds to fairly peaky time patterns.

3.2. Runoff Model

Effective storm rainfall is computed by multiplying rainfall intensity from the catchment idf curves with a runoff coefficient. The runoff coefficient increases with storm depth and approaches a limiting value exponentially. This relationship is based on both the flood frequency simulations in a downward approach (M. Sivapalan et al., unpublished manuscript) and the analysis of a large number of observed events in the pre-alpine Ötscherbach catchment [*Blöschl et al.*, 1995]:

$$r_c = 0.88 - 0.58 \times \exp\left(\frac{-p}{150}\right) \tag{5}$$

where r_c is the runoff coefficient, and p is the storm rainfall depth (in millimeters), which is intensity times duration ($p = it_r$). Runoff is routed by a linear reservoir where the characteristic response time, t_c, is a function of both event runoff depth and catchment area:

$$q_p(T, t_r, A) = q_{\text{ratio}} \times i(T, t_r, A) \times r_c(p)$$

$$\cdot \left(1 - \exp\left(\frac{-t_r}{t_c(r_c p, A)}\right)\right) \tag{6}$$

Here q_p is peak flow (millimeters per hour) of a given return period, T; i is catchment rainfall intensity (millimeters per hour); and t_r is storm duration. The catchment response time, t_c, consists of a hillslope component, t_{hill}, and a channel component, t_{ch}:

$$t_c = t_{hill} + t_{ch} \tag{7}$$

For the hillslope component the response time of the 36-km^2 Ötscherbach catchment is used [*Blöschl et al.*, 1995; M. Sivapalan et al., unpublished manuscript]:

$$t_{hill} = 1 \left/ \left(\frac{\alpha}{8} + \frac{\beta}{30} + \frac{1 - \alpha - \beta}{100}\right)\right. \tag{8}$$

where the weights α and β have been found by calibration for the Ötscherbach catchment:

$$\alpha = 0.50 + 0.00123 pr_c$$

$$\beta = 0.27 + 0.00059 pr_c \tag{9}$$

Units of t_{hill} are hours and units of p are millimeters. Equations (8) and (9) imply faster response for larger events. The channel component, t_{ch}, represents the channel travel times for catchments larger than the 36-km^2 Ötscherbach catchment and has been specified as

$$t_{ch} = A^{0.35} - 3.5 \tag{10}$$

where A is the catchment area (square kilometers) and the units of t_{ch} are hours. The exponent is based on values reported in the literature [e.g., *Pilgrim*, 1987; *Corradini et al.*, 1995] and appears to be suitable for Austrian conditions. For small catchments this relationship gives catchment response times on the order of $t_c = 5$ hours, which is quite a typical value for small rural catchments in Austria. For large catchments of, say, 100,000 km^2 this relationship gives values of about 60 hours, which is a typical value of the Danube at Vienna (catchment area of 102,000 km^2). Finally, a base flow of 0.03 m^3/s/km^2 (i.e., 0.1 mm/h) was added. It should be noted that the runoff model is nonlinear in both the abstractions and the routing component.

3.3. Derived Flood Frequency Framework

The rainfall model and the runoff model have been combined in an analytical framework (Figure 3). Very briefly, in this framework the runoff peaks produced by storms of different durations are weighted by the marginal distribution of storm durations. This allows estimation of the return period for a given flood peak, which gives the flood frequency curve. From this, CV and the mean annual flood were calculated. The derived flood frequency curve was evaluated for return periods from $T = 1.001$ to 1000 years. It should be emphasized that catchment area enters into the model at two points: first through the rainfall model (catchment idf curves) and second through the runoff model (catchment response times) (Figure 3; see also (6), (7), and (10)). CV and mean annual floods calculated with this model are shown in Figure 4 as a function of catchment area. The large squares in Figure 4 indicate the catchments for which the derived flood frequency model has been developed (i.e., Ötscherbach, Mitterbach, or Reith) (M. Sivapalan et al., unpublished manuscript). It is therefore not surprising that for these three catchments, both simulated CV and mean are close to the observations. In fact, most of the parameters used here are those of the Ötscherbach catchment (top markers). The only exception is the spatial scaling of rainfall (i.e., catchment idf curves), which is the reason for the slight underestimation of both CV and mean. The simulated relationships in Figure 4 fall well within the range covered by
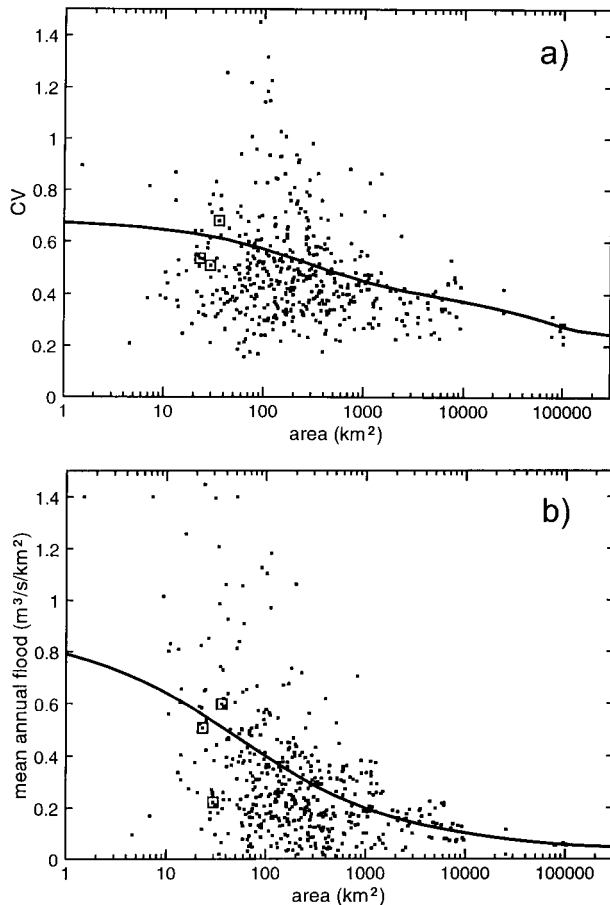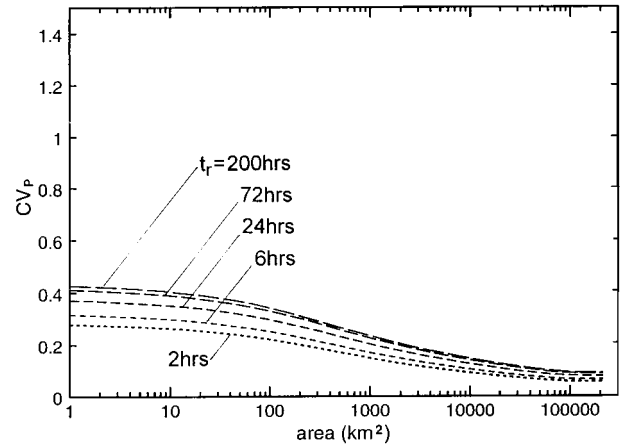

Figure 5. Coefficient of variation (CV_p) of rainfall intensities conditional on duration, t_r, which can be interpreted as conditional CV of runoff for a linear system.

the data. There is a slight trend of decreasing CV with area, which closely resembles the "average" behavior of the data. Similarly, there is a clear decrease in the mean annual floods with area, which is consistent with the data. The good fit of mean annual floods is partly due to the fact that this was one of the criteria used in selecting the spatial correlation structure of precipitation (equation (2)). However, there are two major questions: (1) Why does CV decrease with catchment area? and (2) Can we explain the scatter and, in particular, the extreme values of CV? Motivated by these questions, we start in the following section with a much simpler derived flood frequency model and build up complexity in steps in order to understand the process controls.

4. Interaction of Storm Duration and Catchment Response Time

Figure 5 shows the CV of annual maximum rainfall for various durations plotted versus catchment area based on the catchment idf curves [*Sivapalan and Blöschl*, 1997]. There is a slight decrease of CV with catchment area which is related to the spatial correlation structure of rainfall. There is a slight increase of CV with duration which is related to the shape of the idf curves. Specifically, one can think of it, in a way, as evidence of an "upper limit" of intensity. Short durations will approach that limit since intensities are large, which translates into smaller CVs. On the other hand, large durations do not approach that limit since intensities are smaller, and hence CV is larger. The catchment idf curves are based on a K45-type of rainfall regime [*Schimpf*, 1970], which reflects average conditions in Austria. Also, this type of regime is quite representative of the range of CVs for single station rainfalls: *Seebacher and Shahin* [1985] analyzed 151 stations in Austria, each with 70 years of record, and found a total range of CV of 0.23 to 0.43 for annual maxima of daily rainfall. It is important to realize that the CVs in Figure 5 are conditional on storm duration.

The catchment idf curves have been combined with a linear runoff model with constant runoff coefficient, r_c, and constant catchment response time, t_c:

Figure 4. Coefficient of variation and mean annual floods per unit area as in Figure 1. Solid lines refer to simulations with the derived flood frequency model.

$$q_p(T, t_r, A) = i(T, t_r, A)r_c\left(1 - \exp\left(\frac{-t_r}{t_c}\right)\right) \quad (11)$$

where q_p is peak flow (millimeters per hour) of a given return period, T; i is catchment rainfall intensity (millimeters per hour); and t_r is storm duration. The linear model simply acts as a multiplier on both the mean and the standard deviation of rainfall. Hence the conditional CV of runoff (conditional on t_r) is identical with the conditional CV of rainfall. Figure 5 can therefore be interpreted as representing conditional CVs of runoff applicable for linear systems.

The essence of the derived flood frequency approach is to combine the conditional values of Figure 5 into a single weighted average (G. Blöschl and M. Sivapalan, unpublished manuscript). This has been done in Figure 6 on the basis of the marginal distribution of storm duration (equation (3)) and the simple linear runoff model (equation (11)). CV as a function of catchment area, A, and catchment response time, t_c is shown. Figure 6b presents the information of Figure 6a in a perspective view. For very small values of t_c the CV of runoff approaches that of precipitation, which is clear from (11). The CV of precipitation (solid line with markers in Figure 6a) consists of two parts: (1) the conditional CV shown in Figure 5, which is due to variability in intensity from storm to storm for a given duration, and (2) the variability in storm duration, which translates via the idf curve into variability of intensities. The CV of storm duration is close to 1 (CV = 1.18 in (3)) and hence represents a larger component than conditional CV of intensity. As a consequence of this and because the distribution of storm durations is not a function of catchment area, the unconditional CV of precipitation (solid line with markers in Figure 6a) does not change much with catchment area. The CV of runoff is always smaller than the CV of precipitation. This is due to the dependence of storm intensity on duration, inherent to the idf curve, and the interplay of duration and catchment response time discussed in detail by G. Blöschl and M. Sivapalan (unpublished manuscript). Specifically, the interplay filters out some of the rainfall variability. In fact, if rainfall intensity and duration are assumed to be statistically independent, simulations (not shown here) indicate that the CV of runoff is always larger than the CV of precipitation. This is consistent with the findings of *Robinson and Sivapalan* [1997] who assumed rainfall intensity and duration to be independent.

The interplay between rainfall and runoff model filters out variability in a complex way (Figure 6). Figure 6c (dashed line) shows a cross section through Figures 6a and 6b at a catchment scale of 100 km². CV decreases with catchment response time, t_c, reaches a minimum around t_c = 48 hours, and increases for larger t_c. It is quite clear, as suggested by the case of average storm duration δ = 6 hours (solid line in Figure 6c), that the minimum in CV occurs at a catchment response time equal to the average storm duration. This is reminiscent of the effect of t_c/δ on the ratio of runoff to rainfall return periods demonstrated in Figure 13 of G. Blöschl and M. Sivapalan (unpublished manuscript). Clearly, these findings are closely related and support the conclusion of G. Blöschl and M. Sivapalan (unpublished manuscript) that the dimensionless number t_c/δ is an important control on flood frequency.

Figure 6c also indicates that the CV of runoff increases with average storm duration, δ. This is related to the shape of the idf curves where mean and standard deviation change at different rates, and a smaller CV of storm duration for smaller δ (CV = 0.99 in (3) with δ = 6 hours while CV = 1.18 with δ = 48 hours).

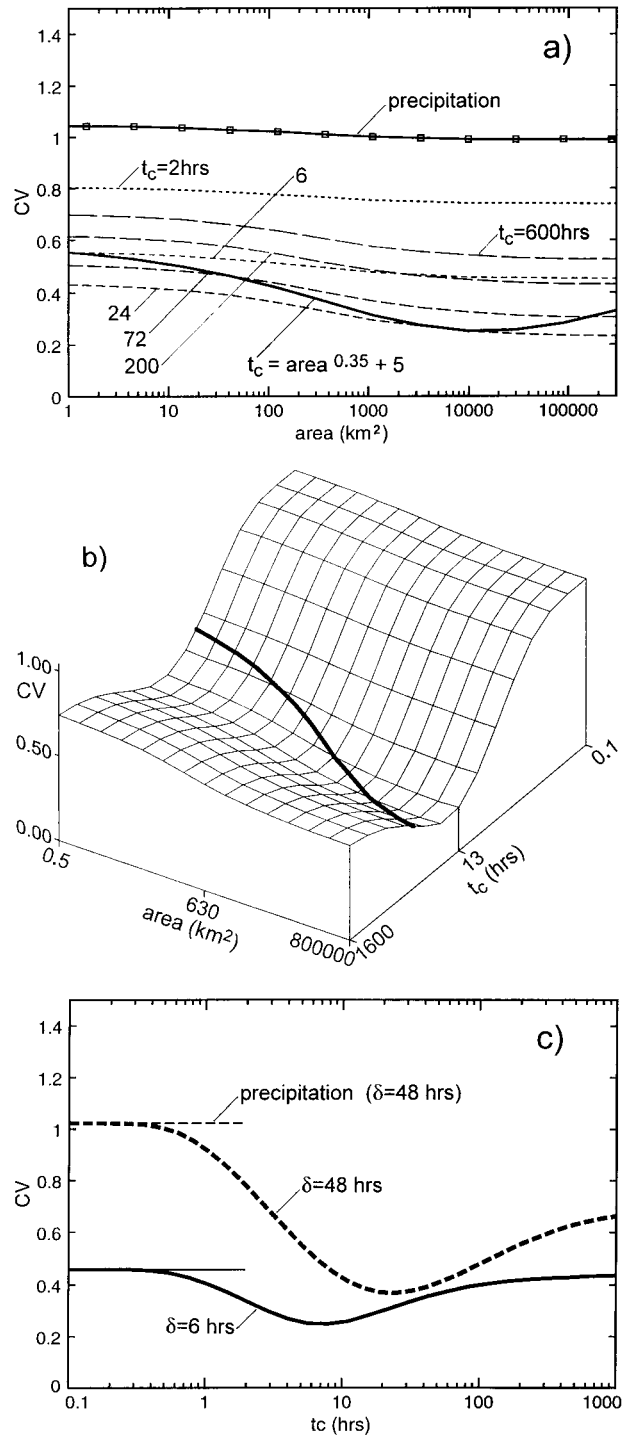The "saddle" shown in Figure 6 appears to occur at all

Figure 6. Coefficient of variation (CV) of runoff computed with a linear runoff model (Equation (11)) as a function of catchment area and catchment response time, t_c. There are no within-storm time patterns; threshold storm duration a = 1.5 hours; average storm duration δ = 48 hours. Solid line with markers in Figure 6a represents CV of precipitation. Thick lines in Figures 6a and 6b show $t_c = A^{0.35} + 5$. Dashed line in Figure 6c represents a cross section through Figures 6a and 6b at a catchment scale of 100 km² and solid line in Figure 6c is for δ = 6 hours.

catchment scales. If we assume a functional relationship between t_c (hours) and catchment area, A (square kilometers),

$$t_c = A^{0.35} + 5 \qquad (12)$$

then the family of curves in Figure 6a reduces to a single curve and the "saddle" translates into a minimum in CV of runoff as a function of catchment scale (thick solid lines in Figures 6a and 6b). This minimum is clearly at variance with data evidence and explanations of other authors. Some authors [e.g., *Gupta and Waymire*, 1990] suggested that the (unconditional) CV of catchment rainfall may decrease with area. For example, *Robinson and Sivapalan* [1997] used a relationship that gave (unconditional) CVs of catchment rainfall of 1.0 and 0.5 for catchment sizes of 1 and 10,000 km², respectively. Given that the (unconditional) CV of catchment rainfall is dominated by the CV of duration, this would imply that the CV of duration actually decreases with catchment area. Physically, this may be related to another aspect of storm-catchment interaction: long duration storms may produce floods both in small and large catchments, while short duration storms are likely not to produce floods in large catchments. This is partly due to initial losses. In larger catchments, at the beginning of a storm, it will take longer to fill up retention capacity because there is more opportunity for retention (e.g., lakes) and because of smaller catchment rainfall intensities. In other words, the duration of flood-producing storms in large catchments may always be larger than some threshold, and the threshold may increase with area. In the approach adopted here, this threshold is represented by the parameter a in (3) for the distribution of storm durations. For illustration, a (hours) was assumed to increase with area, A (square kilometers) according to

$$a = A^{0.35} + 5 \qquad (13)$$

With this relationship CVs of storm duration are 1.11 and 0.77 for catchment sizes of 1 and 10,000 km², respectively, as opposed to a constant value of 1.18 for $a = 1.5$ hours, as used initially. This gives (unconditional) CVs of catchment rainfall of CV = 1.01 and 0.43 for catchment sizes of 1 and 10,000 km², respectively (Figure 7a), which represents a significant decrease with catchment area. The effect of this decrease on the CV of runoff is shown in Figure 7; Figure 7b is a perspective view. As the CV of runoff is always smaller than that of precipitation (for the linear case), CV of runoff clearly decreases with catchment area for a given catchment response time, t_c, as well as for the composite curve. This is very close to the observed trend. However, it should be noted that the relationship in (13) is speculative and requires further work and proper evaluation. Therefore (13) is not used in the sequel. Rather, the initial value of $a = 1.5$ hours is retained.

Another aspect of storm properties is the temporal pattern of within-storm rainfall intensity. So far (Figures 5–7), constant intensity during a storm has been assumed ($q_{\text{ratio}} = 1$). Figure 8 shows the effect of allowing for temporal patterns (equation (4)). As compared to no time patterns (Figure 6), the minimum in CV is shifted towards shorter catchment response times, t_c. While for no time patterns (and $\delta = 48$ hours) the minimum is around $t_c = 48$ hours, for time patterns it is around $t_c = 4$ hours (Figure 8c). This shift is due to the interaction of storm duration and catchment response time, which has been discussed in detail by G. Blöschl and M. Sivapalan (unpublished manuscript). Specifically, they found the maximum ratio of runoff to rainfall return periods, as a func-
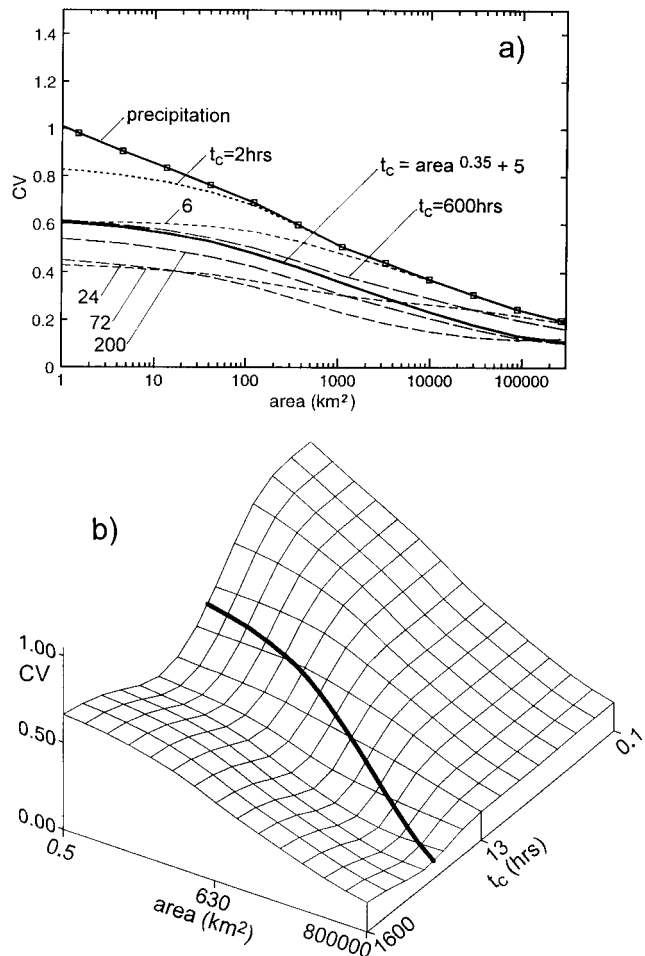

Figure 7. Same as Figure 6 but with threshold storm duration a increasing with area.

tion of t_c, to shift when temporal patterns were included (their Figure 13). Clearly, this is closely related to the effects shown here.

5. Nonlinearity in Runoff Generation

This section examines the effect of nonlinear runoff processes. Specifically, in Figure 9 the same processes as in Figure 8 were considered, but the runoff coefficient, r_c, was assumed to vary with storm rainfall depth (equation (5)), and catchment response time, t_c, was assumed to consist of a hillslope and a channel component (equation (7)). The hillslope component, t_{hill}, is nonlinear according to (8), and various values for the channel component, t_{ch}, are examined. The case of $t_{ch} = 0$ corresponds to $t_c = t_{hill}$, which is on the order of 10 hours (equations (8) and (9)). A comparison of this case in Figure 9 with Figure 8a reveals that the presence of nonlinearity significantly increases the CV of runoff at all catchment scales. For example, at 100 km² the increase is from CV = 0.4 (Figure 8a) to CV = 0.6 (Figure 9). This is not surprising, as the presence of nonlinearity in runoff processes is generally expected to steepen the flood frequency curve (e.g., G. Blöschl and M. Sivapalan, unpublished manuscript). The increase in CV is due to the combined effect of runoff generation (r_c) and runoff routing (α, β). Simulations (not shown here) and the results of
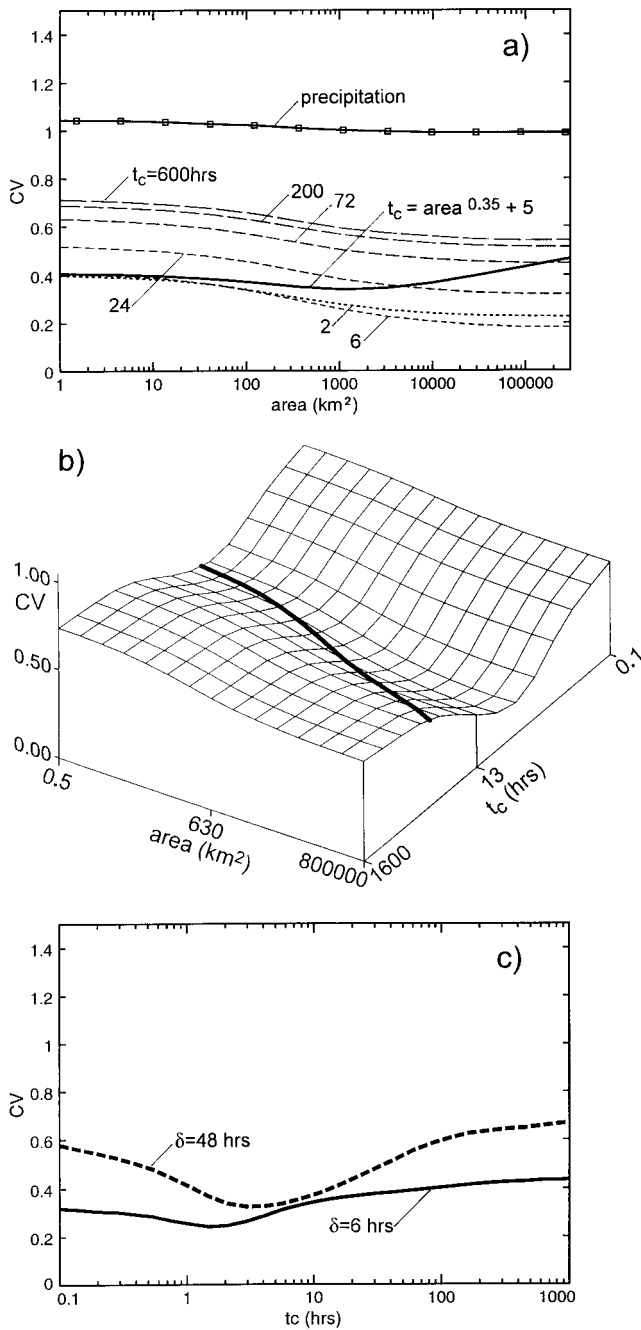
Figure 8. Same as Figure 6 but allowing for within-storm time patterns.

Figure 9. CV of runoff as in Figure 8 but allowing for non-linear runoff generation and nonlinear routing.

ments. This is because for larger catchments, the values of α and β in (9) will be close to the intercepts of 0.5 and 0.27, respectively, and therefore t_c will not vary much with return period. The solid line in Figure 9 shows the composite curve with $t_{ch} = A^{0.35} - 3.5$, which decreases with area for catchment scales smaller than 1000 km^2. The decrease is due to a number of factors, including the scaling of conditional catchment rainfall (Figure 5) and decreasing nonlinearity of runoff processes with catchment scale. Beyond 1000 km^2 the curve increases due to increasing channel response times and the interplay of catchment and rainfall timescales (Figure 8b). The location of the minimum (1000 km^2) is controlled, among other things, by within-storm time patterns, as can be seen by comparing Figures 6c and 8c. The composite curve intersects the curve for $t_{ch} = 0$ at a catchment size of 36 km^2 because this size has been adopted in the approach of splitting catchment response time into a hillslope and a channel component (equation (7)). In fact, the composite curve is identical with that in Figure 4 (and hence the complete model described in section 3) in all components except base flow. Zero base flow has been used in Figure 9.

It is clear from Figure 9 that nonlinear runoff processes are an important mechanism for increasing CV. We will now analyze various types of nonlinearity and examine if they can explain the very large CVs encountered in the data (Figure 1a). Specifically, we will analyze threshold processes that represent a simple form of strong nonlinearity. Threshold behavior refers to a rapid changeover from one state to another. This type of behavior seems to be omnipresent in hydrologic processes, particularly when moving from small to extreme events [*Gutknecht*, 1994]. Examples include the transition from saturation excess to infiltration excess mechanism, subsurface pathways (e.g., macropores or karstic conduits) becoming operative beyond a critical event scale, and the transition from snowfall to rainfall at a threshold air temperature [*Blöschl et al.*, 1991]. We will give an illustration of this more generic problem by examining thresholds in the runoff coefficient as a function of storm depth. Specifically, two cases of a small constant runoff coefficient below a threshold p_1, large constant runoff coefficient above a threshold p_2, and linear behavior in between are used:

$$r_c = 0.3 \qquad p \leq p_1$$

$$r_c = 0.7 \qquad p \geq p_2 \qquad (14)$$

G. Blöschl and M. Sivapalan (unpublished manuscript) indicate that r_c tends to play the more important role.

Figure 9 also suggests that CV increases with channel response time, t_{ch}. This is because catchment response times are such (on the order of 10 to 100 hours) that only the right-hand side of the "saddle" in Figure 8c (dashed line) comes into play (also see Figures 8a and 8b). Furthermore, Figure 9 indicates, for a constant value of t_{ch} (dashed lines), that CV decreases faster with catchment scale than in the linear case. Partly, this is due to generally higher values of CV. Partly, this is due to lower catchment rainfall intensities in larger catchments, which, with the type of nonlinearity chosen, translate into less nonlinear behavior and hence smaller CVs in larger catch-
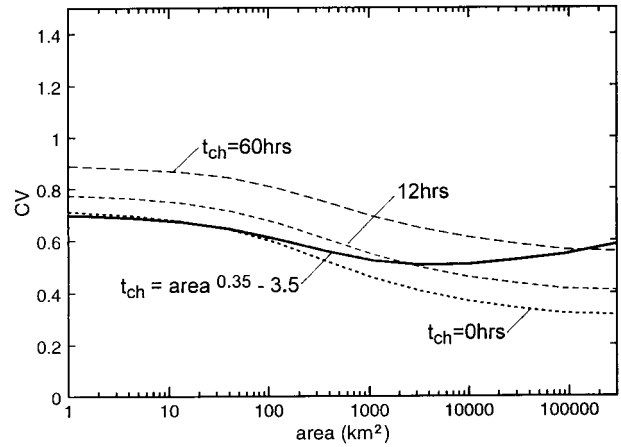
$$r_c = 0.3 + 0.4 \frac{p - p_1}{p_2 - p_1} \qquad p_1 < p < p_2$$

where r_c is the runoff coefficient and p is event rainfall depth (millimeters). One of the cases uses $p_1 = 100$ mm and $p_2 = 150$ mm (case 100/150), and the other case uses $p_1 = 150$ mm and $p_2 = 200$ mm (case 150/200). The third case represents a step increase as

$$\begin{array}{ll} r_c = 0.3 & p \le p_3 \\ r_c = 0.9 & p > p_3 \end{array} \qquad (15)$$

where $p_3 = 200$ mm (case 200/200). The same model parameters as those in Figure 9 ($t_{ch} = 0$, dotted line) are used except for the runoff coefficient. The results are shown in Figure 10a. For catchment scales smaller than 100 km², CV increases significantly with the strength of nonlinearity. The largest CVs (up to CV = 1.1) are produced by case 200/200 (equation (15)) which represents a very strong nonlinearity indeed. The linear case shown in Figure 10a (constant runoff coefficient $r_c =$
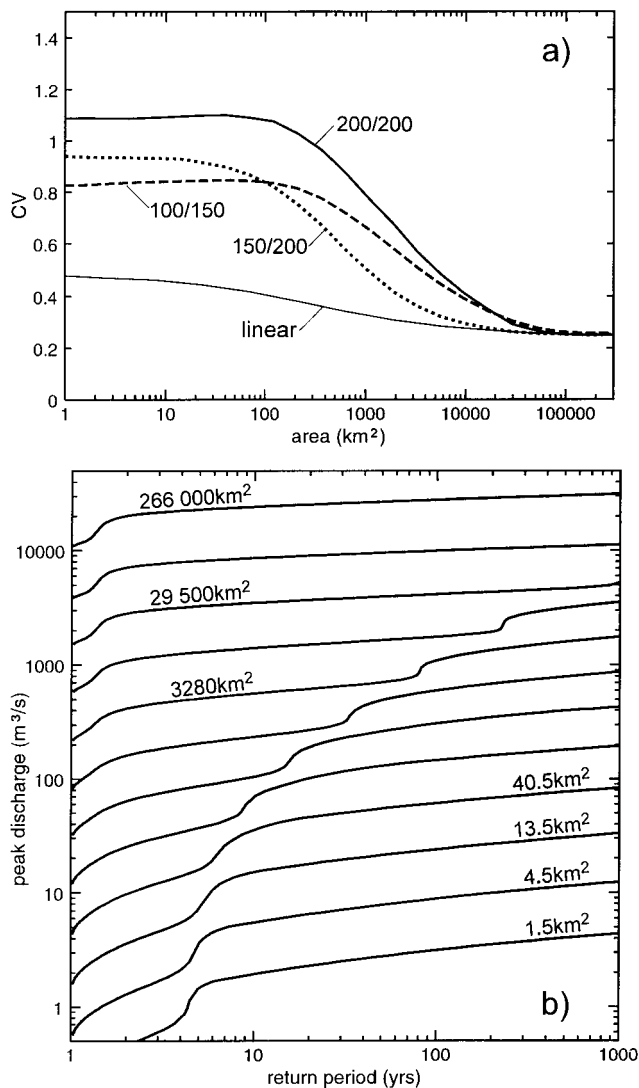

Figure 11. Effect of sampling on CV for case 150/200 of Figure 10a. Error bars refer to the range of CV from 10 realizations of 40 years each.

Figure 10. (a) Effect on CV of thresholds in runoff coefficient. A linear case (constant runoff coefficient $r_c = 0.3$) is given for comparison. (b) Flood frequency curves for case 150/200 in Figure 10a; $t_{ch} = 0$.
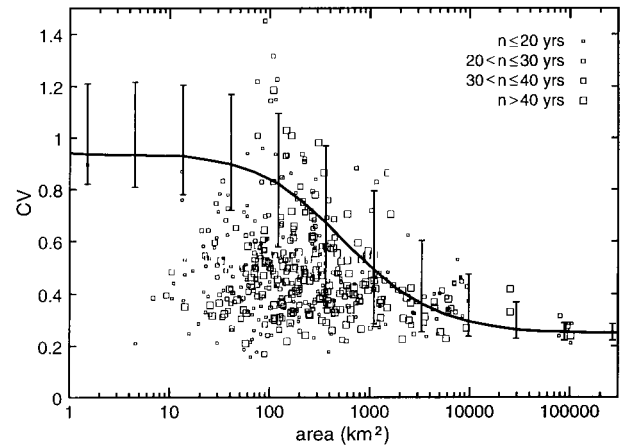
0.3) gives much lower CVs (around CV = 0.4). The effect of nonlinearity is clearly consistent with the findings of Figure 9. Around 100 to 1000 km², however, CV rapidly decreases with area and reaches a constant value of about 0.25 at very large catchment scales. To interpret these results, the flood frequency curves for case 150/200 have been plotted in Figure 10b. The most striking features in Figure 10b are the "kinks" in the flood frequency curves, which are a consequence of the threshold in runoff coefficient. Similar kinks have been reported by G. Blöschl and M. Sivapalan (unpublished manuscript), and a discussion is provided there. The interesting thing here is that the kink appears to move towards larger return periods with increasing catchment size. This is due to decreasing catchment rainfall intensities with catchment scale, for a given return period, and a constant threshold in (14). In other words, in larger catchments large return periods are required to exceed the threshold; hence the kink in Figure 10b appears at large return periods. With increasing catchment scale the kink moves away from the mean annual flood ($T = 2.3$ years), which makes it contribute more to CV. This is the reason for the slight increase of CV between 1 and 100 km² (Figure 10a). At about 10,000 km² the kink moves beyond the maximum return period evaluated ($T = 1000$ years), and what remains is a flood frequency curve due to an essentially constant runoff coefficient. This is the reason for the rapid decrease of CV with catchment size and the small CVs at large catchment scales.

The importance of the maximum return period evaluated naturally leads to the question of sampling. To assess the effect of sampling, we performed the following analysis. We treated the derived flood frequency curve as the parent cumulative distribution function of flood peaks. For each catchment scale we drew 40 random samples of flood peaks (representing 40 years of record) from the flood frequency curve (Figure 10b; case 150/200 in Figure 10a) from which we calculated sample CVs. This was repeated 10 times, representing 10 realizations (i.e., 10 catchments). The range of CV calculated for the 10 realizations was plotted as error bars for each catchment size in Figure 11. The solid line represents the "true" pattern of CV (i.e., the parent distribution from Figure 10a). The error bars are generally large. This means that for this type of parent distribution, the CV cannot be computed very reliably from
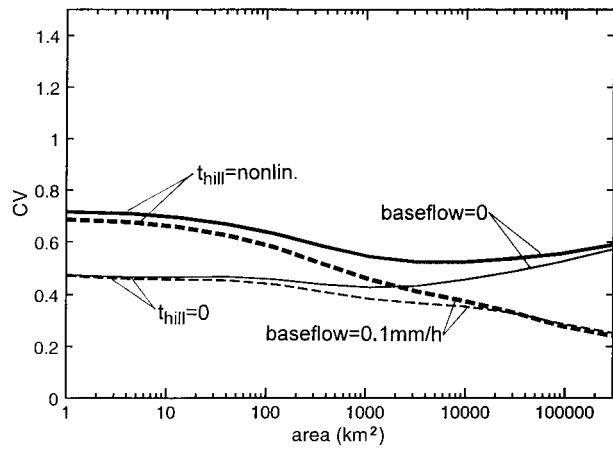
Figure 12. Effect on CV of base flow as a surrogate of seasonality.

observed flood peaks. It should be noted that the assumption of 40 years of record being available in the sampling exercise is a favorable case. Most records of the data set are shorter, which means that the error bars may be even larger. The maximum CVs observed (CV ≈ 1.5) stem from catchments with less than 30 years of record and can therefore be easily explained in terms of runoff generation along with the sampling problem (Figure 11). More generally speaking, it may well be that a considerable part of the scatter in observed CVs is due to sampling. The error bars appear to be largest at the catchment scale where CV decreases rapidly with area (100 to 1000 km^2). This is clear from Figure 10b. At that catchment scale an extreme event (beyond the kink) may or may not be "observed" within the 40 years of record of the sampling exercise, depending on the realization (i.e. catchment). This gives a plausible interpretation of "outliers" as floods beyond the "kink" in the flood frequency curve. The error bars are smallest at large catchment scales as, there, the flood frequency curves are smooth and outliers never occur during the 40 years of record.

6. Hydrologic Regimes

So far, we have examined individual process controls. In real catchments a number of processes are operative simultaneously, but their relative importance will differ from catchment to catchment. It is therefore useful to analyze typical combinations of processes. We choose the concept of hydrologic regimes to quantify the overall catchment behavior in a holistic way. Regimes are unique in their combination of processes, while in a single process, there may be overlap with other regimes. This idea can perhaps be best illustrated by an example from anthropology, where an ethnic group is unique in its combination of customs, language, social views, etc., while a single aspect may well coincide with another group. We adopt the classification of hydrologic regimes according to *Kresser* [1981], shown in Figure 2, which focuses on the seasonality of mean streamflow. The seasonality of mean streamflow has an important connection with the seasonality of flood behavior. For example, in regimes I to III, which are glacier and snow dominated, flows are always high in summer and floods generally also occur in summer. This means that the base flows of large floods are always fairly large. Similar connections exist for the other regimes. Base flow, in fact, may be interpreted as a surrogate for other processes such as snowmelt and seasonality in rainfall processes, and this is the way we will use it in the simulations.

Figure 12 shows the effect on CV of including base flow of 0.1 mm/h (i.e., 0.03 m^3/s/km^2). Adding base flow always decreases CV because the mean annual flood is increased while the standard deviation remains constant. This effect is particularly pronounced at larger catchment scales where the mean annual floods are smaller, and hence the relative contribution of base flow is larger. The case of linear routing ($t_{hill} = 0$) without base flow gives increasing CVs with catchment scale due to increasing channel response times and the interplay of storm duration and catchment response time (Figure 8). If base flow is included (Figure 12), there is a significant decrease with catchment area for large catchments. The case of nonlinear routing and no base flow (Figure 12) shows a slight minimum at 1000 km^2 due to the effects discussed for Figure 9. If base flow is included, there is a clear decrease of CV with catchment scale for all catchment sizes. It should be noted that base flow per unit area is likely not to be uniform in space. This may cause some additional scatter in CV.

Clearly, a number of processes are important, and the actual patterns of CV will depend on their relative importance. This is examined by using typical parameter combinations for the regimes in Figure 2. The parameter values (Table 1) are based on a judgment of important runoff processes and an analysis of streamflow records of those catchments that are given in Figure 2. For each regime, three cases are considered to cover the likely range of CV. Case "low" refers to parameter combinations that should produce relatively low CVs, case "high" refers to high CVs, and case "fast" refers to relatively fast runoff response. The regimes are only applicable to a limited range of catchment sizes, which is indicated in Table 1.

Table 1. Parameters for Regimes in Figure 2 used for Figure 13

Regime	Base Flow, mm/h			Hillslope Response Time, t_{hill}, hours			Channel Response Time, t_{ch}			Runoff Coefficient			Catchment Size, km^2
	Low	High	Fast	Low	High	Fast	Low	High	Fast	Low	High	Fast	
I	0.60	0.30	0.60	Öt + 30	Öt	6.5	(1)	(1)	(1)	Öt	Öt	Öt	<3000
III	0.10	0.05	0.20	Öt + 30	Öt	9.5	(1)	(1)	(1)	Öt	Öt	Öt	<30000
IV	0.02	0.007	0.007	Öt	Öt	4.5	(1)	(1)	(1)	Öt	100/150	50/100	<10000
V	0.05	0.05	⋯	1000	300	⋯	(1)	(1)	⋯	0.8	0.8	⋯	<3000
VI	0.15	0.10	0.15	Öt	Öt	0	(1)	(1)	(2)	Öt	Öt	Öt	>300

For hillslope response times, "Öt" refers to nonlinearity according to (8) and (9). For channel response times, (1) refers to $t_{ch} = A^{0.35} - 3.5$ and (2) refers to $t_{ch} = A^{0.30}$. For runoff coefficients, "Öt" refers to nonlinearity according to (5); 100/150 and 50/100 refer to p_1/p_2 in (14). For other parameters, within-storm time patterns are according to (4). Marginal distribution of storm duration is according to (3).
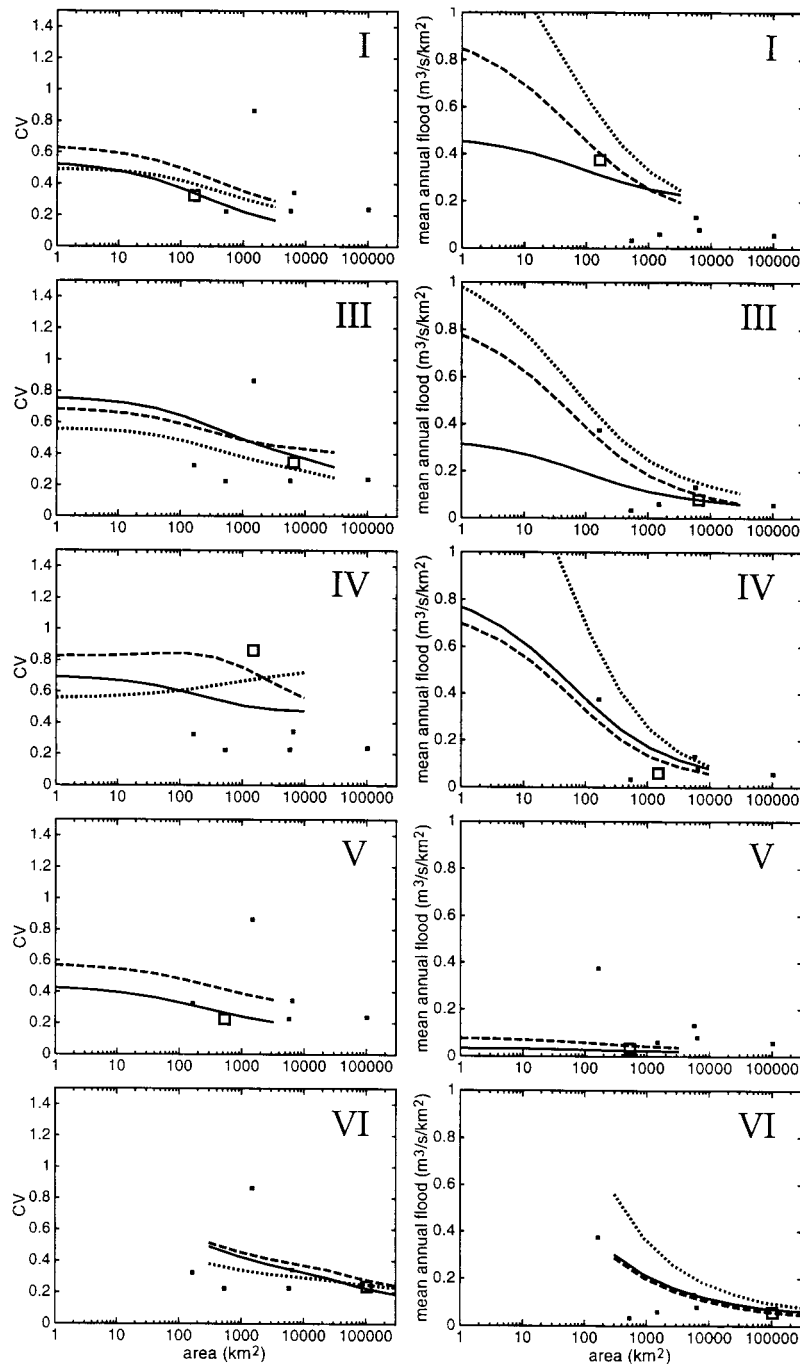
Figure 13. CV and mean annual floods per unit area for the regimes of Figure 2 with three parameter combinations of Table 1 (solid line, low; dashed line, high; dotted line, fast). Points are the observed values for the catchments in Figure 2 and large squares refer to the catchments representative of a particular regime.

CVs and mean annual floods for the regimes calculated with the parameters of Table 1 are shown in Figure 13. Mean annual floods always decrease with catchment scale, while there are various shapes for CV. The differences between regimes are smaller in terms of CV than in terms of mean annual floods. The points in Figure 13 refer to observed CVs and mean annual floods of the catchments in Figure 2, and the large squares represent the catchments that are representative of a particular regime. Regime I (glacier dominated) gives a consistent decrease of CV with catchment area, which is mainly due to having used base flow as a surrogate for season-

ality. Results for regime III (snow dominated) are similar, but the decrease is less pronounced owing to smaller base flows. Regime II is in between regimes I and III and has not been plotted. Regime IV represents streams from prealpine foothills and hilly terrain, where floods can occur at any time of the year and runoff processes may be highly nonlinear. In Figure 13 this is reflected in a complex pattern of CV with generally large CVs and a tendency of CV to increase with catchment scale (Figure 10a). One of the cases (case "high," dashed line) shows a slight increase in CV with catchment scale for small catchments and a maximum at 100 km², which are mainly
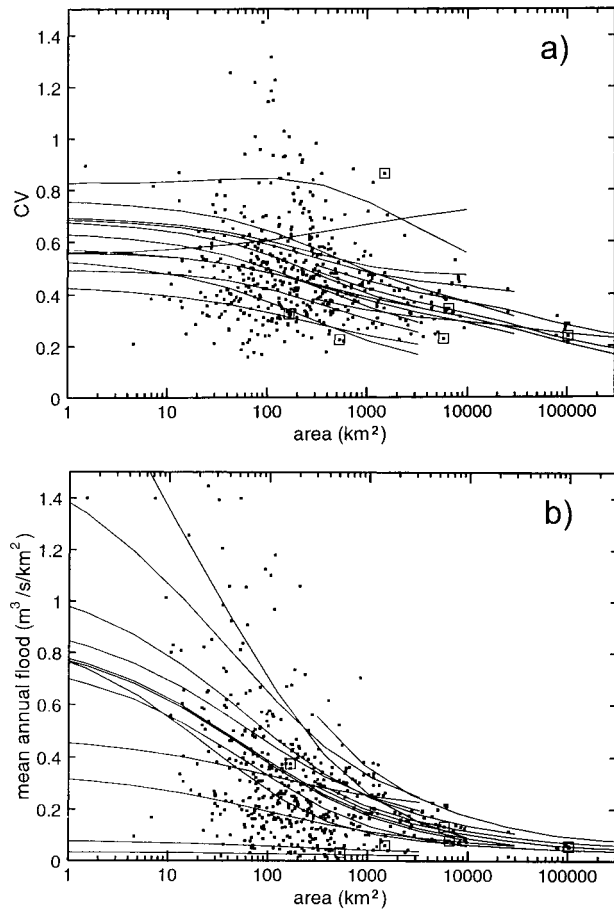
Figure 14. CV and mean annual floods per unit area of Figure 13 combined into one plot with full data set of Figure 1.

Table 2. Summary of Process Controls on CV of Runoff and the Relationship Between CV and Catchment Area

Process	Case	Parameter	CV	CV = f(area)	Figure
CV of catchment rainfall conditional on duration, t_r		···	···	−	5
Dependence of rainfall intensity, i, and duration, t_r		···	−	···	6a
Interplay of catchment response time, t_c, and storm duration, t_r	$t_c < \delta$ $t_c > \delta$	t_c	− +	···	6a, 7a, 8a
Average storm duration		δ	+	···	8a
Effective storm duration larger than threshold time, a		a	−	−	6b, 7b
Channel response time, t_{ch}, = f(area)	$t_{ch} < \delta$ $t_{ch} > \delta$	··· ···	··· ···	− +	6a, 7a
Within-storm time patterns		q_{ratio}	−	+	6c, 7c
Nonlinear runoff generation (changing r_c with event scale)		···	+	−	9
Nonlinear runoff routing (changing α, β with event scale)		···	+	−	9
Threshold processes (below and above threshold area, A_{th})	$A < A_{th}$ $A > A_{th}$	··· ···	+ −	+ −	10
Base flow (seasonality of snow and glacier melt)		baseflow	−	−	12, 13
Base flow (all regimes)		baseflow	−	−	12, 13

Pluses refer to an increase and minuses to a decrease of CV due to the parameter or a process (column "CV"); or to an increase/decrease of CV as a function of catchment area (column "CV = f(area)"). Figure numbers refer to those figures where process controls are discussed. Assessment gives tendency of process controls and interplay of processes is discussed in the text.

due to increasing channel response times (see Figures 8b and 12). On the other hand, runoff response from groundwater-dominated streams (regime V) is very slow, and hence mean annual floods are very low. However, this is only partly reflected in CV. The main reason why CVs are smaller here than in other regimes is that runoff processes may be very linear (Table 1). Finally, regime VI (large river basins) shows a composite behavior, where most factors point to a decrease of CV with catchment area. All of the regimes give CVs and mean annual floods that are close to the sample catchments (large squares).

The regimes of Figure 13 have been combined into a single plot in Figure 14. With the range of CVs obtained and considering the sampling problem (see Figure 11), the simulations nicely cover the scatter of observed CVs. In fact, the simulations reveal hidden patterns behind the apparent scatter. It is clear from Figure 14a that the notion of an "average" behavior of CV is probably not very useful, as there is no physical basis for it. Rather, what appears as a center line in Figure 4 is the superposition of many patterns, each of which is controlled by specific hydrologic processes. Similar comments apply to mean annual floods (Figure 14b).

7. Discussion and Conclusions

On the basis of a derived flood frequency model, the process controls on the relationship between CV of maximum annual floods and catchment scale has been examined. A summary of the results is given in Table 2, which is based on Figures 5–13. Specifically, Table 2 shows whether a process tends to increase (plus sign) or decrease (minus sign) the CV. Also shown is whether a process tends to give rise to an increase or decrease of CV with catchment scale. There is roughly an equal number of processes that increase CV and processes that decrease CV. However, most processes, but not all, point to a decrease of CV with catchment area. Clearly, there is a complex interplay between individual processes. At the core of process controls appears to be the interaction of catchment response time, t_c, and storm duration, t_r, but the magnitude is not large, and often this interaction is hidden by other processes. The dependence of rainfall intensity and duration is clearly very important and reduces CV significantly. While CV of catchment rainfall conditional on duration gives rise to only a slight decrease with catchment scale of CV of runoff, a potential change of the distribution of effective rainfall durations with catchment area may be important. This requires further analysis. Increasing channel travel times with catchment scale tend to translate into increasing CVs with area. Nonlinear runoff processes, including threshold effects, are the main mechanism for increasing CV. They give rise to complex patterns in the relationship between CV and area. Base flow has been used as a surrogate for a number of processes, such as seasonality of

streamflow. It decreases CV for all regimes and, in particular, leads to a significant decrease of CV with area.

The various process controls very well explain the observed behavior of CV in 489 Austrian catchments. Observed CVs show a tendency to decrease with area which is what most processes do. Also, the range of CVs observed can be explained by the model. Very large CVs may be due to nonlinear runoff generation processes, in particular, threshold behavior, along with the sampling problem. This means that very large CVs may be partly due to short observation periods. Very small CVs may be explained by seasonality of streamflow (represented by base flow here) and linearity of runoff processes due to groundwater contributions. It appears that much of the variability of CV between catchments is due to runoff processes rather than to rainfall variability. This is suggested by the relatively small range of conditional CVs of rainfall data (0.23 to 0.43) [*Seebacher and Shahin*, 1985]. However, the effect of variability in storm durations (and hence unconditional CVs; Figure 7) as well as variability in storm types (and hence intensity-duration relationships) may be important. This needs further examination.

It is clear that there is no unique explanation of the observed relationship between CV of runoff and catchment scale. Rather, both the tendencies and the scatter are due to a combination of complex patterns, each of which can be explained by a number of alternative process controls. It is also clear that catchment area is not the most important control on regional CV. The dependence on area mainly comes from the complex interplay between processes and their relative importance under a given regime.

It appears that the explanations of the relationship between CV and catchment scale suggested in the literature are too simplistic. Although for specific cases they may hold, there is no evidence from this analysis that these explanations have any general validity. *Smith* [1992] hypothesized that the peak of CV as a function of area in the Appalachian data is either a sampling artifact or is related to the organization of extreme storm rainfall and the downstream development of the channel/floodplain system. There are a multitude of other processes suggested in this study (e.g., nonlinearity in runoff generation processes) that may equally well explain the apparent presence of a peak. *Gupta and Dawdy* [1995] suggested that for small catchments, CV may increase with catchment scale owing to basin response. However, results of this study indicate that CVs do not necessarily increase with catchment scale and that both runoff and rainfall processes are important at small scales. Similarly, *Gupta and Dawdy* [1995] suggested that at large catchment scales, CV is mainly controlled by precipitation. It is shown here that this indeed is an important factor. However, other processes such as seasonality of streamflow and channel response times may also be important. *Robinson and Sivapalan* [1997] suggested that the increase in CV in small catchments is due to the interaction between rainfall and catchment timescales. Although this is correct for the assumptions of *Robinson and Sivapalan* [1997], results of this analysis indicate that other processes may be vastly more important, and the effect suggested by *Robinson and Sivapalan* [1997] may never appear in real catchments.

The simulations carried out in this study have placed us in some awe of the complexity of the patterns of CV and their process controls. It is clear that there are consistent patterns behind the apparent scatter of the data. It is therefore important to be wary of generalizations in terms of average statistically estimated trends plus random scatter. It appears more useful to us, as one way to quantify this complexity, to consider typical process combinations, for example, in terms of hydrologic regimes. In practice, the data set of the Austrian catchments used here would probably have been subdivided into a number of homogeneous regions. Both the concept of regimes and the process studies presented here may help delineate such regions in a physically consistent way. Indeed, the main advantage of the derived flood frequency approach used here is to make the interactions and the relative importance of processes transparent rather than to give accurate estimates of CV. Specifically, in the context of the index flood approach this study does give evidence of a tendency for CV to decrease with area. However, this is not the main point. Rather, the results and the approach presented here may help in a careful selection of homogeneous regions for applying the index flood method. They may also help adopt alternative measures of the index flood other than the mean annual flood. Clearly, an approach based on regimes also has major implications for the estimation of extreme floods.

Future work will focus on some of the aspects identified in this study. Specifically, the spatial scaling of effective rainfall duration and within-storm time patterns appears important. The spatial correlation structure of rainfall used here (equation (2)) should be more solidly based on data and rainfall process considerations. Also, a more in-depth analysis of individual regimes appears to be warranted, both in an application-oriented context of design and a more theoretical context of the scaling behavior of hydrologic fluxes [*Blöschl and Sivapalan*, 1995]. It may also be useful to look at the behavior of CV in terms of distance between catchments.

References

Blöschl, G., Scale and scaling in hydrology (Habilitationsschrift), in *Wiener Mitteilungen, Wasser-Abwasser-Gewässer*, vol. 132, 346 pp., Tech. Univ. of Vienna, Vienna, 1996.

Blöschl, G., and M. Sivapalan, Scale issues in hydrological modelling: A review, *Hydrol. Process.*, *9*, 251–290, 1995.

Blöschl, G., D. Gutknecht, and R. Kirnbauer, Distributed snowmelt simulations in an Alpine catchment, 2, Parameter study and model predictions, *Water Resour. Res.*, *27*, 3181–3188, 1991.

Blöschl, G., D. Gutknecht, and A. Watzinger, Design flood for the Erlaufklause dam (in German), Inst. für Hydraul., Tech. Univ. of Vienna, Vienna, 1995.

Corradini, C., F. Melone, and V. P. Singh, Some remarks on the use of GIUH in the hydrologic practice, *Nordic Hydrol.*, *26*, 297–312, 1995.

Cunnane, C., Factors affecting choice of distribution for flood series, *Hydrol. Sci. J.*, *30*, 25–36, 1985.

Dalrymple, T., Flood frequency methods, *U.S. Geol. Surv. Water Supply Pap.*, *1543-A*, 11–51, 1960.

Eagleson, P. S., Dynamics of flood frequency, *Water Resour. Res.*, *8*, 878–898, 1972.

Gelhar, L. W., *Stochastic Subsurface Hydrology*, 390 pp., Prentice-Hall, Englewood Cliffs, N. J., 1993.

Gumbel, E. J., *Statistics of Extremes*, Columbia Univ. Press, New York, 1958.

Gupta, V. K., and D. R. Dawdy, Physical interpretations of regional variations in the scaling exponents of flood quantiles, *Hydrol. Process.*, *9*, 347–361, 1995.

Gupta, V. K., and E. Waymire, Multiscaling properties of spatial rainfall and river flow distributions, *J. Geophys. Res.*, *95*(D3), 1999–2009, 1990.

Gupta, V. K., O. J. Mesa, and D. R. Dawdy, Multiscaling theory of flood peaks: Regional quantile analysis, *Water Resour. Res.*, *30*, 3405–3421, 1994.

Gutknecht, D., Extremhochwässer in kleinen Einzugsgebieten, *Oesterr. Wasserwirtsch. Abfallwirtsch.*, *46*, 50–57, 1994.

Gutknecht, D., and A. Watzinger, Untersuchungen zur Erfassung und quantitativen Abschätzung von abflußrelevanten Faktoren bei der Ermittlung von Katastrophen-Hochwasserereignissen in kleinen Einzugsgebieten (<200 km^2), Inst. für Hydraul., Tech. Univ. of Vienna, Vienna, 1995.

Huff, F. A., Time distribution of rainfall, *Water Resour. Res.*, *3*, 1007–1018, 1967.

Klemeš, V., Conceptualisation and scale in hydrology, *J. Hydrol.*, *65*, 1–23, 1983.

Klemeš, V., Probability of extreme hydrometeorological events—a different approach, in *Extreme Hydrological Events: Precipitation, Floods and Droughts*, *IAHS Publ.*, *213*, 167–176, 1993.

Kölla, E., Zur Abschätzung von Hochwassern in Fliessgewässern an Stellen ohne Direktmessungen, *Mitt. VAW*, *87*, 163 pp., ETH Zürich, Zürich, 1986.

Kresser, W., Die wasserwirtschaftlichen Verhältnisse in Österreich, in *Schriften des Vereines zur Verbreitung naturwissenschaftlicher Kenntnisse in Wien*, pp. 69–97, Vienna, 1981.

Pilgrim, D. H. (Ed.), *Australian Rainfall and Runoff*, vol. 1, 3rd ed., Inst. of Eng., Barton, Australia, 1987.

Robinson, J. S., and M. Sivapalan, An investigation into the physical causes of scaling and heterogeneity in regional flood frequency, *Water Resour. Res.*, *33*, 1045–1059, 1997.

Schimpf, H., Untersuchungen über das Auftreten beachtlicher Niederschläge in Österreich, *Oesterr. Wasserwirtsch.*, *22*, 121–127, 1970.

Seebacher, F. S., and M. M. A. Shahin, Beitrag zur statistischen Auswertung extremer Tagesniederschläge in Österreich, *Oesterr. Wasserwirtsch.*, *37*, 181–190, 1985.

Singh, V. P. (Ed.), Regional flood frequency analysis, in *Proceedings of the International Symposium on Flood Frequency and Risk Analysis*, 400 pp., D. Reidel, Norwell, Mass., 1987.

Sivapalan, M., and G. Blöschl, Transformation of point rainfall to areal rainfall: Intensity-duration-frequency curves, *J. Hydrol.*, in press, 1997.

Smith, J. A., Representation of basin scale in flood peak distributions, *Water Resour. Res.*, *28*, 2993–2999, 1992.

Vanmarcke, E., *Random Fields: Analysis and Synthesis*, 382 pp., MIT Press, Cambridge, Mass., 1983.

Wundt, W., Die größten Abflußspenden in Abhängigkeit von der Fläche, *Wasserwirtschaft*, *40*, 59–64, 1950.

––––––––––––
G. Blöschl, Institut für Hydraulik, Gewässerkunde und Wasserwirtschaft, Technische Universität Wien, Karlsplatz 13/223, A-1040 Vienna, Austria.

M. Sivapalan, Centre for Water Research, University of Western Australia, Nedlands, W. A. 6907, Australia.